European Journal of Immunology
Clinical·Basic·Translational

Immunity to infection

Clinical

Research Article

Immune signature of patients with cardiovascular disease predicts increased risk for a severe course of COVID-19

Manina Günter[*1,2], *Karin Anne Lydia Mueller*[*3], *Mathew J. Salazar*[2], *Sarah Gekeler*[3], *Carolin Prang*[3], *Tobias Harm*[3], *Meinrad Paul Gawaz*[3] *and Stella E. Autenrieth*[1,2]

[1] Department of Hematology, Oncology, Clinical Immunology and Rheumatology, University Hospital Tuebingen, Eberhard Karls University Tuebingen, Tuebingen, Germany
[2] German Cancer Research Centre, Research Group Dendritic Cells in Infection and Cancer, Heidelberg, Germany
[3] Department of Cardiology and Angiology, University Hospital Tuebingen, Eberhard Karls University Tuebingen, Tuebingen, Germany

Severe acute respiratory syndrome coronavirus type 2 (SARS-CoV-2) infection can lead to life-threatening clinical manifestations. Patients with cardiovascular disease (CVD) are at higher risk for severe courses of COVID-19. So far, however, there are hardly any strategies for predicting the course of SARS-CoV-2 infection in CVD patients at hospital admission. Thus, we investigated whether this prediction is achievable by prospectively analysing the blood immunophenotype of 94 nonvaccinated participants, including uninfected and acutely SARS-CoV-2-infected CVD patients and healthy donors, using a 36-colour spectral flow cytometry panel. Unsupervised data analysis revealed little differences between healthy donors and CVD patients, whereas the distribution of the cell populations changed dramatically in SARS-CoV-2-infected CVD patients. The latter had more mature NK cells, activated monocyte subsets, central memory CD4$^+$ T cells, and plasmablasts but fewer dendritic cells, CD16$^+$ monocytes, innate lymphoid cells, and CD8$^+$ T-cell subsets. Moreover, we identified an immune signature characterised by CD161$^+$ T cells, intermediate effector CD8$^+$ T cells, and natural killer T (NKT) cells that is predictive for CVD patients with a severe course of COVID-19. Thus, intensified immunophenotype analyses can help identify patients at risk of severe COVID-19 at hospital admission, improving clinical outcomes through specific treatment.

Keywords: Cardiovascular disease · Immune signature · Immuno-response · SARS-CoV-2 infection · Spectral flow cytometry

Additional supporting information may be found online in the Supporting Information section at the end of the article.

Correspondence: Prof. Stella E. Autenrieth
e-mail: stella.autenrieth@dkfz.de

[*]These authors contributed equally to this work.

Introduction

Coronavirus disease 2019 (COVID-19) is a broad spectrum of clinical manifestations caused by severe acute respiratory syndrome coronavirus type 2 (SARS-CoV-2). Disease severity is related to age, sex, and pre-exiing comorbidities, which impact the immune response during infection [1, 2]. While some individuals experience no symptoms, others face fatal outcomes. Non-severe cases typically prompt a robust, transient immune response, while severe cases entail hyperactive immune cells, excessive cytokine production, and elevated SARS-CoV-2 antibodies [3–6]. Common complications among hospitalised patients include pneumonia, sepsis, acute respiratory distress syndrome, and respiratory failure [7]. Early in SARS-CoV-2 infection, pro-inflammatory cytokines surge, potentially leading to hyperinflammation and subsequent vascular issues, multi-organ failure, and death [8].

Cardiovascular disease (CVD) involves alterations in inflammatory mediators like C-reactive protein (CRP), platelet and monocyte activation, and endothelial and immune cell changes, crucial for atherogenesis and its progression [9, 10]. Elevated cytokine levels recruit inflammatory cells like monocytes, macrophages, and dendritic cells, contributing to atherosclerotic lesions [9]. Additionally, pro-inflammatory adaptive immune cells like Th1 and Th17 play roles in CVD [11–13], increasing the risk of severe SARS-CoV-2 infection [14]. The heightened pro-inflammatory and pro-thrombotic immune response in CVD patients with COVID-19 can lead to myocarditis, acute coronary syndrome, and respiratory complications, resulting in increased mortality [15–18].

Identifying high-risk CVD patients prone to severe COVID-19 remains a challenge, highlighting the need to understand immune system dysfunctions underlying severe cases. We aimed to identify immune system components predicting a severe course of COVID-19 in CVD patients. We comprehensively analysed innate and adaptive immune cells and cytokines in the peripheral blood of SARS-CoV-2-infected or uninfected CVD patients using a 36-color spectral flow cytometry panel and a bead-based immune assay, respectively. Our findings revealed a specific immune signature associated with COVID-19 severity in CVD patients, offering potential predictive value upon hospital admission.

Results

Clinical characteristics of patients with cardiovascular disease and symptomatic acute SARS-CoV-2 infection

We prospectively studied a cohort of 94 nonvaccinated participants from February to April 2020 consisting of 20 CVD patients and 37 CVD patients with symptomatic acute SARS-CoV-2 infection. Thirty-seven healthy donors (HD) served as controls. The baseline characteristics and demographics of the overall cohort are given in Table S1. The population's median age was 58 (IQR 42–74) years, and 45 (47.9%) patients were men. No differences regarding cardiovascular risk factors and co-morbidities were found between CVD patients with and without SARS-CoV2 infection (Table S2). The CVD patients with SARS-CoV2 infection had typical signs of infection, such as fever, cough, dyspnea, and acute respiratory distress syndrome. Out of 37 CVD$^+$SARS-CoV-2 patients, 20 showed respiratory failure with Horovitz index $\leq$ 200 mmHg, while 11 (29.7%) were admitted to the ICU due to progressive respiratory, circulatory, or multi-organ failure. Fourteen CVD$^+$SARS-CoV-2 patients developed a bacterial co-infection during their hospital stay. Laboratory parameters like CRP, high-sensitive Troponin I, lactate dehydrogenase, and aspartate-aminotransferase were significantly elevated in CVD+SARS-CoV-2 compared with CVD patients (Table S2). Their ISARIC-WHO-4C-mortality-score further stratified CVD$^+$SARS-CoV-2 patients into a group of expected mild, moderate, or severe course of COVID-19 (Table S3 (https://isaric4c.net/risk/)). Patients with expected mild COVID-19 were significantly younger ($p = 0.016$) than those with moderate or severe disease course. Cardiovascular risk factors were equally distributed among the three groups, whereas laboratory parameters like lymphocyte count, CRP, and IL-6 levels showed significant alterations (Table S3).

Characterisation of immune cell subsets in peripheral blood using a 36-colour spectral flow cytometry panel

Frozen peripheral blood mononuclear cells (PBMCs) from the described patient cohort were stained with a 36-colour antibody panel (Fig. S1) related to a previously published panel [19] and measured with a spectral flow cytometer to characterise all common immune cell subsets (Fig. 1A). Data analysis was performed classically by manual gating (Fig. S2) as well as by unsupervised analysis using a Uniform Manifold Approximation and Projection (UMAP) [20] for dimensionality reduction followed by clustering using a self-organised map (FlowSOM) [21] (Fig. 1C). UMAP plots show differences between the concatenated files of the different cohort groups (Fig. 1B). Unsupervised data analysis revealed the discrimination of 40 manually annotated specific cell populations reflecting the manual gating strategy (Fig. S2). These cell populations include B cells (lilac), CD4$^+$ (orange) and CD8$^+$ T cells (blue), NK cells (green), monocytes (pink), dendritic cell subsets (violet), innate lymphoid cells (ILCs, light green) and CD161$^+$ T cells (turquoise), as well as basophils (yellow) and neutrophils (purple).

Differences in the abundance and phenotype of immune cell populations in SARS-CoV2-infected compared with uninfected CVD patients

Next, we assessed the differences in the abundance of the 87 MCs obtained by FlowSOM (annotated to 40 different cell populations as described in Fig. 1) in PBMCs from HD and CVD patients with and without SARS-CoV2 infection (Fig. S4). Comparison of HD and uninfected CVD patients revealed a reduced frequency

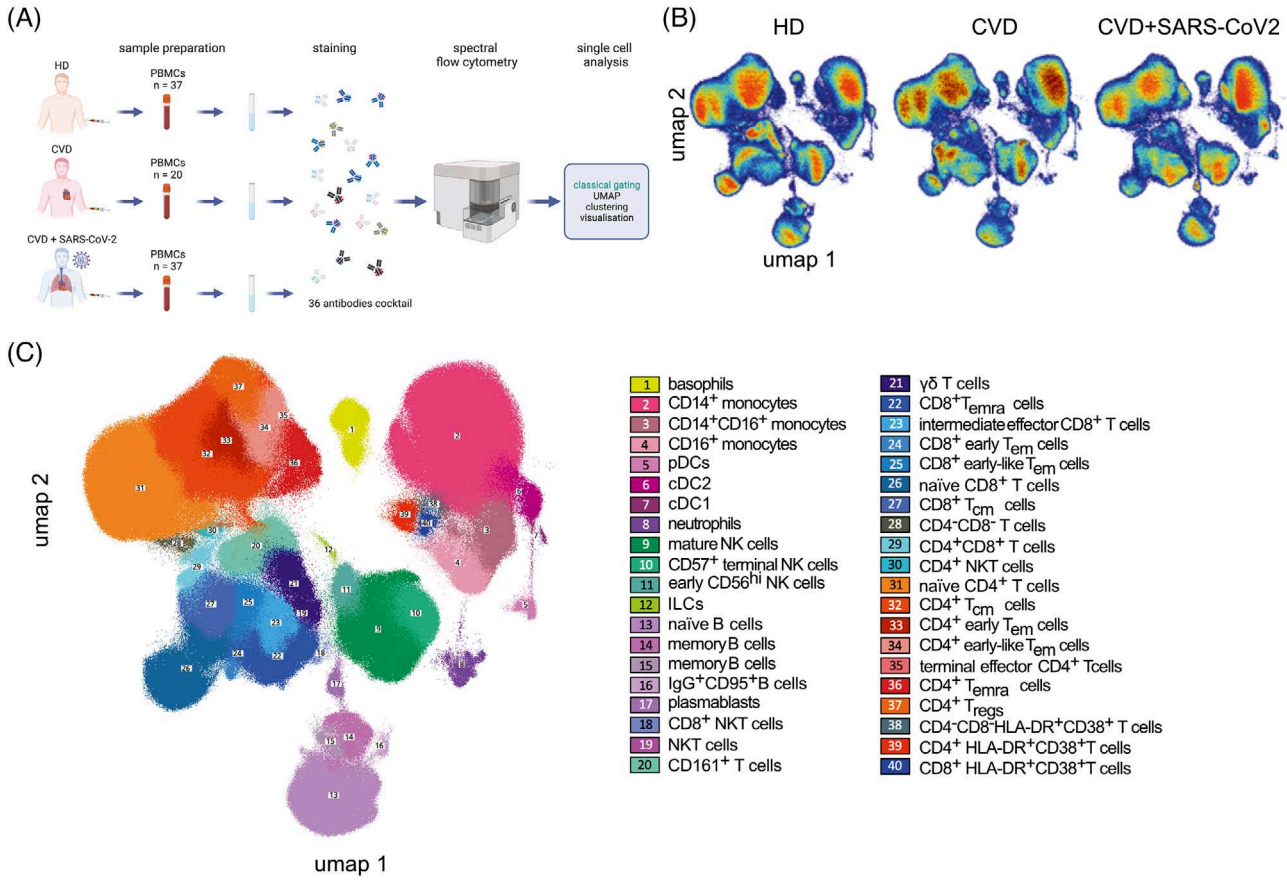

Figure 1. UMAP dimensional data analysis of PBMCs using a 36-colour antibody panel. (A) Clinical and experimental design of the study (B) UMAP projection of PBMCs from healthy donors (HD, 37), CVD patients (CVD, 20), and CVD patients with SARS-CoV-2 infection (CVD + SARS-CoV2 patients, 37). The density plots show concatenated events from all of the indicated samples. (C) 40 FlowSOM clusters projected onto two UMAP dimensions of concatenated events from all samples. FlowSOM clusters were assigned to depicted cell populations based on their marker expression.

of cells in clusters assigned to γδ T cells [22], Mucosal-associated invariant T cells [23], naïve $CD8^+$ T cells, early-like effector memory $CD4^+$ T cells ($CD4^+$ early-like T_{em}), $CD4^-CD8^-$ T cells, and naïve B cells in CVD patients. In contrast, clusters corresponding to innate inflammatory cells like $CD14^+$ monocytes, neutrophils [24], mature NK cells, and $CD8^+$ central memory T cells ($CD8^+$ T_{cm}) showed increased cell frequencies in CVD patients compared with HD (Fig. S5).

SARS-CoV-2-infected CVD patients revealed significantly more mature NK cells, $CD14^+CD16^+$ monocytes, plasmablasts, and activated populations of $CD14^+CD45RA^+$ monocytes, $CD38^+CD4^+$ T_{cm} cells, and $HLA\text{-}DR^+CD38^+PD\text{-}1^+CD8^+$ early T_{em} cells compared with uninfected CVD patients (Fig. 2B). In contrast, a reduced proportion of innate lymphoid cells (ILCs), conventional dendritic cell (cDC) subsets cDC1 and cDC2, $CD16^+$ monocytes, and less activated or mature populations of $CD14^+$ monocytes, $CD4^+CD8^+$ T cells, naïve, central memory, early effector-memory $CD8^+$ T cells and $CD4^+$ T_{regs} were observed in SARS-CoV2-infected compared with uninfected CVD patients (Fig. 2). To complement our unsupervised analysis, we performed a manual gating strategy (Fig. S2), which yielded comparable results at the cell number level (Fig. S6). Additionally, fewer T helper 17 (Th17), follicular T helper cells, and γδ T cells were detected after SARS-CoV-2 infection.

In addition to changes in the proportion of immune cells, SARS-CoV-2-infected CVD patients showed phenotypical changes compared with uninfected CVD patients (Fig. S7). Innate immune cells were more activated, as NK cell subsets expressed CD38, CD95, and CCR5 more. Plasmacytoid DCs, important in viral infections due to their type I interferon response [25], displayed increased CCR7, CD38, and CD95 expression, and ILCs expressed more CXCR3 or CD45RA, CD28, and CD25.

In contrast, the cDC subsets from SARS-CoV-2-infected CVD patients showed less expression of HLA-DR and CD38 but increased expression of CCR5, CCR7, CD11b, CD45RA, and IgG (cDC2s) (Fig. S7), indicating cellular activation and migration, but also reduced antigen presentation capacity. Similarly, all monocyte subsets showed increased CCR7 expression, whereas HLA-DR, CD38, and CD45RA expression was reduced. Most strikingly, we found an enhanced expression of the thrombin receptor CD141 on monocyte clusters from SARS-CoV-2-infected patients, possibly alluding to impaired blood coagulation [26].

Adaptive immune cell populations displayed a more inhibitory phenotype in SARS-CoV2-infected CVD patients compared with

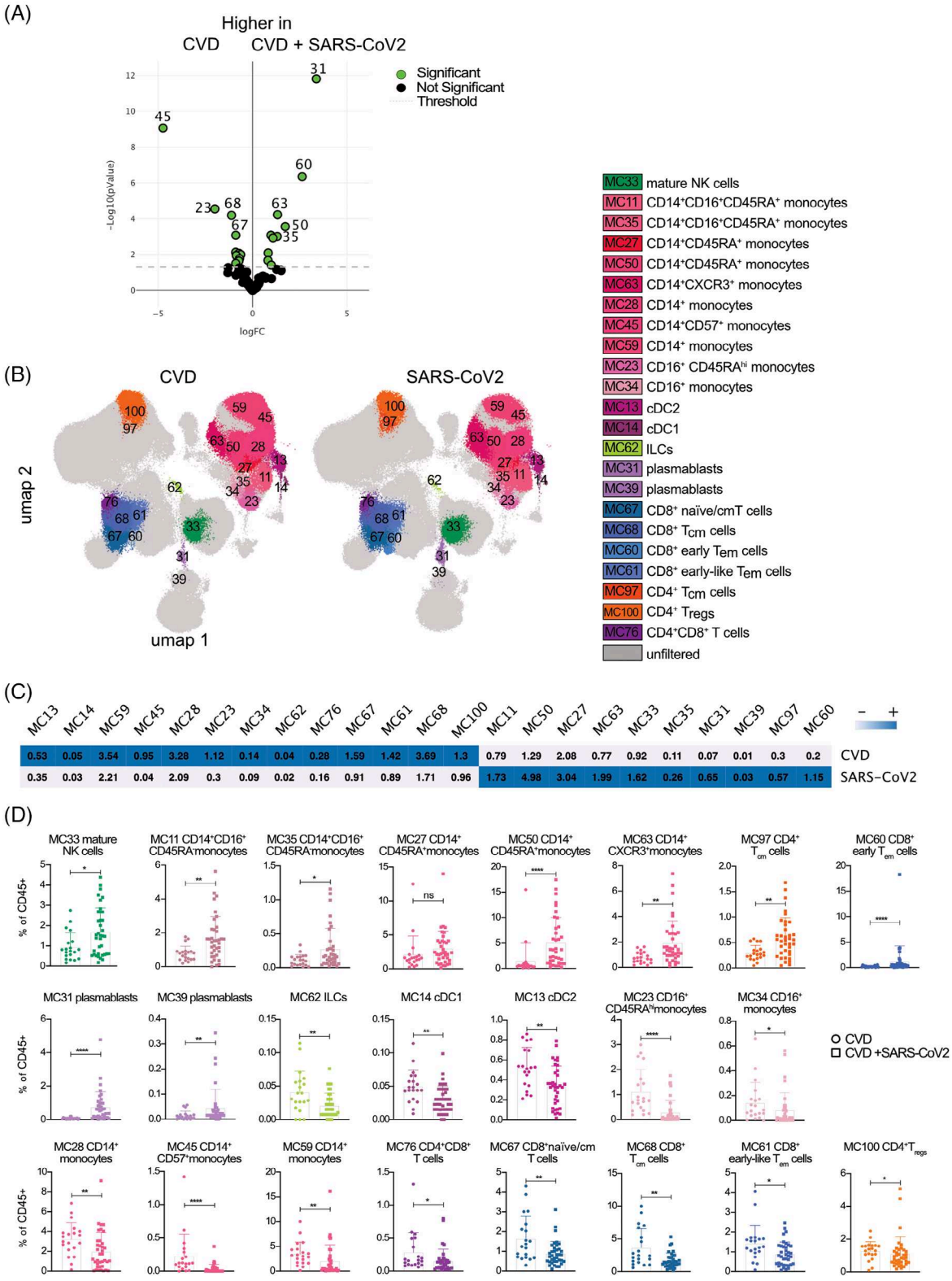

Figure 2. Differences between immune cell populations of CVD patients compared with SARS-CoV2-infected CVD patients. (A) Volcano plot comparing the frequency of cells in 87 FlowSOM clusters using edgeR. Significant clusters are depicted in green used in (B)–(D); FC = fold change. (B) UMAP overlay plot shows concatenated events from the two groups of a. (C) Clustered heatmap displaying the frequency of cells in the FlowSOM clusters. (D) Box plots show the abundance of the depicted MC with assigned cell populations of the individual samples. Data were analysed using multiple Mann–Whitney non-parametric tests with a false discovery rate. Significant differences between the two patient cohorts are marked with stars (* <0.05; ** <0.01; *** <0.001; **** <0.0001).

uninfected (Fig. S7). The only exception was the plasmablasts showing reduced expression of the apoptotic marker CD95 combined with increased CD38 expression, indicating a more functional and long-living phenotype. B-cell subsets were characterised by lower CD38, HLA-DR, CCR6, CD45RA, and IgD expression. $CD8^+$ and most $CD4^+$ T-cell subsets showed increased expression of the activation marker CD38, increased expression of inhibitory molecule PD-1, and less expression of the co-stimulatory molecule CD28 and CXCR3. This hints towards an impaired migratory and T-cell activation capacity of $CD4^+$ and $CD8^+$ T-cell subsets [27]. In summary, our data show an infection-induced activation of innate immune cells in combination with reduced numbers and inhibitory phenotypes of DCs and adaptive immune cells.

Significant differences in chemokine and cytokine profiles between SARS-CoV-2-infected and uninfected CVD patients

Plasma levels of 25 common cytokines and chemokines were analysed in HD and SARS-CoV-2-infected and uninfected CVD patients. As shown previously, pro-inflammatory cytokines IL-6 and IL-18 were significantly increased in SARS-CoV-2-infected compared with uninfected CVD patients and HD (Fig. S8A) [28, 29]. TNF, IL-1β, IL-12p70, IL-23, and IL-33 levels were lower in SARS-CoV-2-infected compared with uninfected CVD patients and HD, whereas CCL2 and the CXCR3 ligands CXCL9, CXCL10, and CXCL11 were elevated during SARS-CoV-2 infection. These data indicate increased recruitment of monocytes (CCL2), NK, $CD4^+$ Th1, and $CD8^+$ T cells (CXCR3 ligands), in combination with impaired cell proliferation (IL-1b, TNF) and T-helper cell differentiation (IL-12, IL-33, IL-23) in SARS-CoV-2-infected CVD patients. Furthermore, IL-6 and IL-8 were significantly increased in severe compared with mild SARS-CoV2-infected CVD patients, whereas CCL17, responsible for the recruitment of T cells link [27], was significantly less abundant in severely infected CVD patients (Fig. S8B). Correlation analysis revealed significant associations within the subgroups of SARS-CoV-2-infected, mainly CXCL9 with CXCL10 and IL-10 with IFN-γ, and uninfected CVD patients with high correlations of IFN-α, IL-10, IL-12p40, IL-17A, and TNF-α (Fig. S8C).

An immune signature of SARS-CoV-2-infected CVD patients is associated with the severity of COVID-19

To determine an association between immune signatures and COVID-19 severity, the abundance and alterations of immune cell populations of CVD patients with expected mild, moderate, or severe course of COVID-19, classified by their ISARIC WHO 4C-Mortality-Score, were analysed.

Comparing the frequencies in the above-defined 87 MC from patients with mild and severe or moderate and severe courses of COVID-19 revealed 19 significantly different MCs among the groups (Fig. 3A, Fig. S9). These comprised reduced frequencies and numbers (Fig. S10) of neutrophils, $CD161^+$ T cells, $HLA\text{-}DR^{hi}CD14^+$ monocytes, and IgG^+CD95^+ B cells in severe compared with mild SARS-CoV-2-infected CVD patients. In contrast, a more significant proportion of mature NK cells, $CD45RA^+CD14^+$ monocytes, $CD8^+$NKT cells, and several $CD4^+$ and $CD8^+$ T-cell subsets, including $CD4^-CD8^-HLA\text{-}DR^+$ T cells, naïve $CCR6^+CXCX3^+CD4^+$ T cells, central memory, and effector subsets was detected (Fig. 3).

Phenotypical changes included, for example, less CD19 expression on MC representing naïve and memory B cells in severe compared with mild and/or moderate SARS-CoV2-infected CVD patients, indicating less B-cell receptor signalling [30] (Fig. S11). Similarly, CD16 expression was lower on neutrophils, monocyte subsets, mature NK cells, NKT cells, $CD8^+$ T_{em} and T_{emra} cells, and $CD4^+$ T_{cm} cells from severe COVID-19, indicating less antibody-dependent cellular toxicity and thereby less killing of virus-infected cells (antibody-dependent cellular cytotoxicity [31]). Accordingly, in CVD patients with a severe course of COVID-19, $CD14^+CD16^+$ monocytes expressed less HLA-DR and neutrophils, mature NK cells, $CD161^+$ T cells, and several clusters representing $CD4^+$ naïve, T_{cm} and T_{em} cells less CXCR3 (Fig. S11).

Thus, severe SARS-CoV-2 infection resulted in fewer innate immune cells. Although an increased proportion of NK cells, $CD4^+$, and $CD8^+$ T-cell subsets were observed in CVD patients with severe COVID-19, their expression of functional markers like CD16 and CXCR3 was impaired, indicating an altered immune response in this subgroup.

Immune signature is predictive of severity of SARS-CoV-2 infection in CVD patients

We then sought to identify an immune signature that could predict the course of SARS-CoV2 infection when hospitalised. We used a combination of immune cell populations (unsupervised data analysis), which showed differences when comparing CVD patients with mild and severe SARS-CoV-2 infection or with moderate and severe SARS-CoV-2 infection (Fig. 4A). In mildly infected SARS-CoV-2 CVD patients, more neutrophils, $CD161^+$ T cells and IgG^+CD95^+ B cells were found, whereas severely infected patients had more NKT cells, plasmablasts, $CD4^-CD8^-HLA\text{-}DR^+$ T cells and $CD4^+$ Temra cells (Fig. 4A). When comparing the moderately infected patients with the severely infected patients, the intermediate effector $CD8^+$ T cells, $CD8^+$ NKT cells, and cDC2 were higher in moderately SARS-CoV-2-infected CVD patients (Fig. 4A and B).

Next, to identify subjects with pre-existing CVD who developed severe COVID-19, we searched for combinations of immune cell populations (immune signature). For this purpose, we used the recently published CombiROC package [32]. This analysis tool uses combinatorial analysis and ROC curves to accurately determine the optimal combination of markers from different omics methods to predict differences between two groups. For this anal-

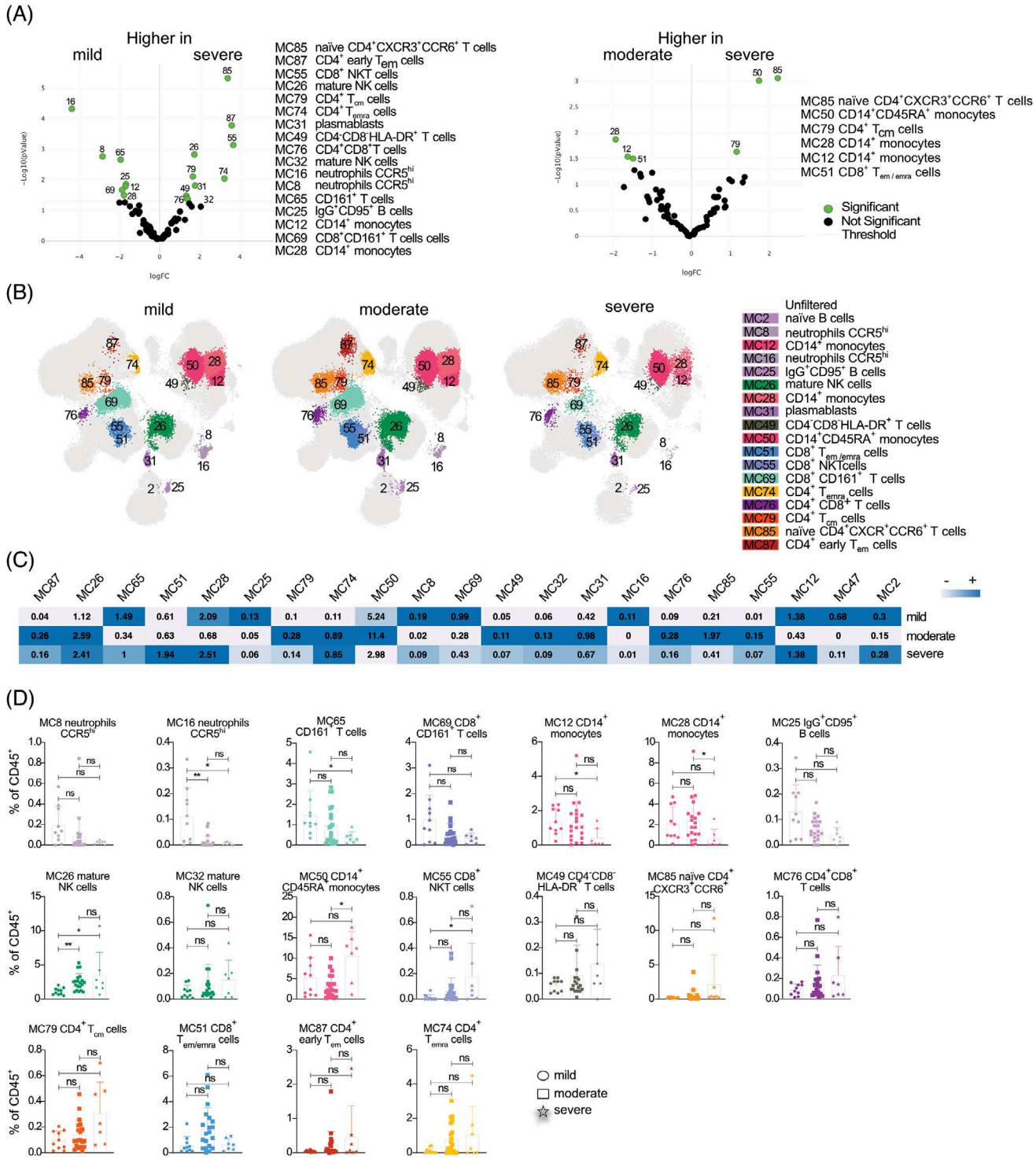

Figure 3. Differences between immune cell populations in mild, moderate, and severe SARS-CoV2-infected CVD patients. (A) Volcano plots comparing the frequency of cells in the 87 FlowSOM clusters from mild [10], moderate [20], and severe [7] SARS-CoV2-infected CVD patients using edgeR. Significant different clusters are depicted in green and used in (B)–(D). (B) The UMAP overlay plot shows concatenated events from the three groups of (A). (C) The clustered heatmap displays the frequency of cells in the FlowSOM clusters. (D) Box plots show the abundance of the depicted MC with assigned cell populations of the individual samples. Data were analysed using the Kruskal–Wallis nonparametric test with Dunn's post-test. Significant differences between the patient cohorts are marked with stars (* <0.05; ** <0.01; *** <0.001).

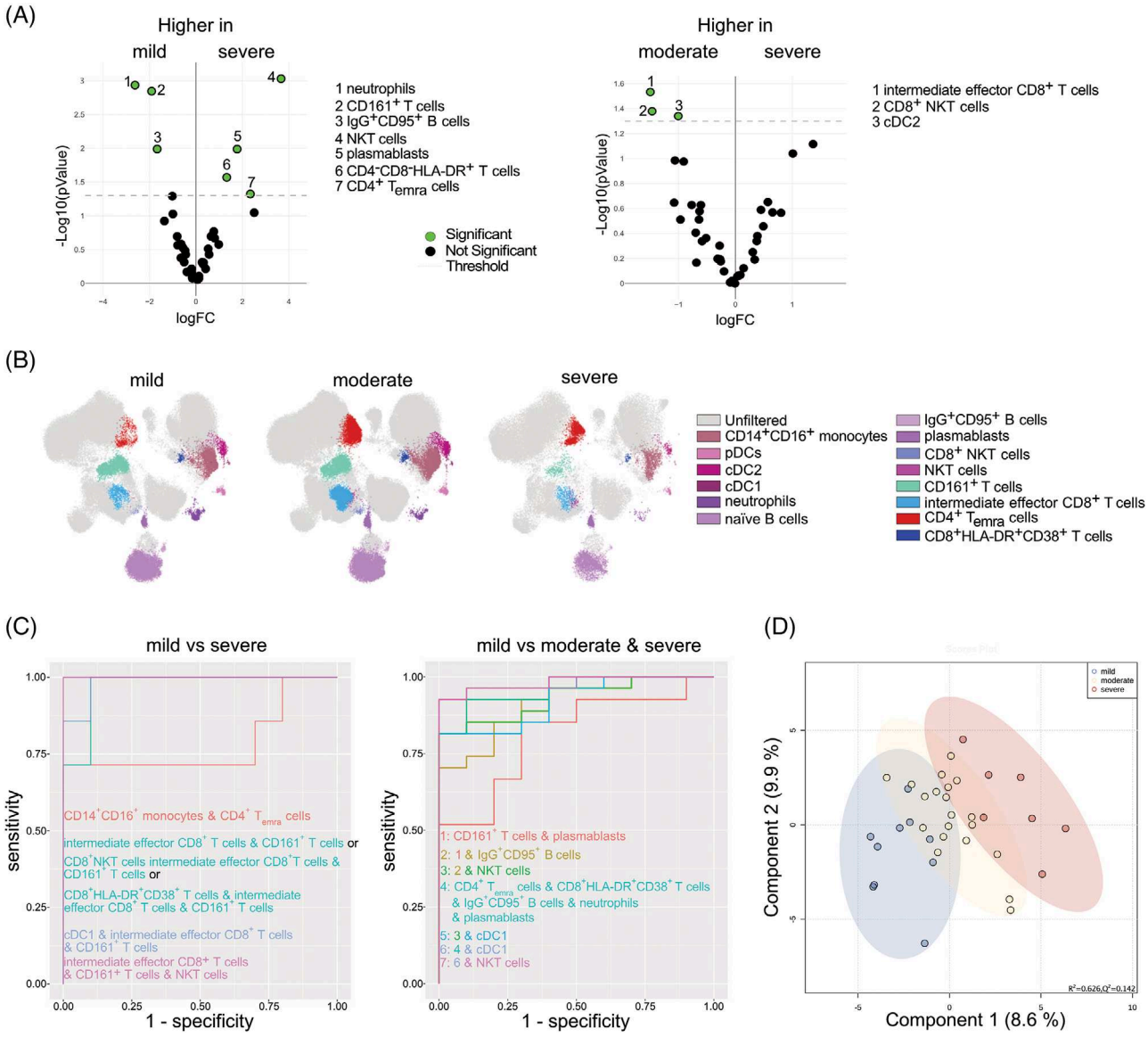

Figure 4. Correlation of immune cell abundance with disease severity. (A) Volcano plot comparing the cell frequencies of 40 assigned cell populations (from Fig. 1) from mild [10], moderate [20], and severe [7] SARS-CoV2-infected CVD patients using edgeR. Significantly different cell populations are depicted in green and used in (B) and (C). (B) UMAP overlay plot shows concatenated events from the three groups of (A). (C) CombiROC analysis comparing significantly different cell populations (from (A)) from patients with mild and severe (left) or mild and the combination of moderate and severe course of infection (right). (D) OPLS-DA comprising immune cell populations and cytokine/chemokine plasma levels of patients with SARS-CoV2 infection. Dots represent single study subjects and are coloured by disease severity (mild = blue, moderate = yellow, severe = red points). X- and Y-axis shows the T score and percentage of explained variance.

ysis, we have selected these immune cell populations that differ in abundance in the different cohorts of patients as described above. The combination of CD161$^+$ T cells, intermediate effector CD8$^+$ T cells, and NKT cells predicted a severe compared with a mild course of disease in SARS-CoV-2 infected CVD patients at hospital admission with a sensitivity and specificity of 1 (pink line) (Fig. 4C; Table S5). A combination of CD4$^+$ T_{emra}, CD8$^+$HLA-DR$^+$CD38$^+$ T cells, IgG$^+$CD95$^+$ B cells, neutrophils, plasmablasts, cDC1, and NKT cells is required to predict a mild versus moderate or severe course of infection (Fig. 4C; Table S6).

To illustrate the importance of different immune parameters in patients with different severity of infection, an orthogonal partial least squares discriminant analysis (OPLS-DA) was performed [33], including all immune cell populations and cytokine/chemokine plasma levels of SARS-CoV-2 infected CVD patients. The enormous impact of altered immune signatures on clinical disease progression is indicated by the large variance between patients with mild (blue) and severe (red) infections (Fig. 4D). In contrast, PLS-DA analyses, including the immunological parameters of the entire cohort, showed no clear separation

of patients by baseline characteristics (i.e. age, sex, BMI, diabetes mellitus, or smoking, Fig. S12–S13), suggesting that the impact of the immune signature on clinical disease progression is substantial.

In conclusion, using high-resolution flow cytometry, we identified an immune cell combination consisting of $CD161^+$ T cells, intermediate effector $CD8^+$ T cells, and NKT cells that stratified CVD patients at high risk of severe SARS-CoV2 infection on the day of hospital admission.

Discussion

Our study identified a characteristic immune signature in patients with CVD and acute, symptomatic SARS-CoV-2 infection that predicts a severe course of COVID-19. In contrast to previous studies, we focused on patients with pre-existing CVD who are at high risk of developing progressive cardiopulmonary failure as a result of the infection [14, 15, 34]. Most other studies that examined immune cell populations in the blood of SARS-CoV-2 infections did not stratify their analyses by comorbidities [4, 5, 35–41]. Furthermore, these studies did not consider the expected severity of COVID-19 by association with established risk scores.

Compared with HD, a chronic pro-inflammatory response in CVD patients might lead to a more pronounced immune response to viral infections such as SARS-CoV-2. Consistent with and in addition to previous studies, we observed changes in the frequencies of innate immune cells like $CD14^+$ monocytes, neutrophils, mature NK cells, and $CD161^+$ T cells, and the adaptive immune cells $CD4^+CD8^+$, $CD8^+$ naïve and central memory T cells, γδ T cells, early-like effector memory $CD4^+$ T cells, and naïve B-cell subsets in CVD patients compared with HD [9, 13, 42]. Moreover, IL-6 levels were increased in CVD patients compared with HD.

SARS-CoV-2 infection activates innate immune cells, reduces their number, and induces inhibitory phenotypes of DCs and adaptive immune cells in CVD patients. For example, in agreement with other studies, we show fewer non-classical monocytes in peripheral blood. These cells migrate to the site of organ injury, where they maintain the inflammatory processes [36, 41, 42]. In addition, in SARS-CoV-2 infection, a higher proportion of mature NK cells, $CD14^+CD16^+$ monocytes, activated populations of $CD14^+CD45RA^+$ monocytes, plasmablasts, $CD4^+$HLA-DR^+CD38^+ and $CD8^+$HLA-$DR^+CD38^+PD\text{-}1^+$ cells [4, 5, 35, 37, 40, 41], while ILCs, dendritic cell subsets cDC1 and cDC2, less activated/mature $CD14^+$ monocytes and $CD8^+$ T-cell subsets were reduced [4, 5, 35, 40, 41, 43].

SARS-CoV-2-infected CVD patients also showed some phenotypic changes, the most important of which are briefly discussed here, such as higher expression of CD38 on plasmablasts, monocytes, NK cells, and T-cell subsets [37, 39, 41, 44] less HLA-DR on antigen-presenting cells [4, 39, 41, 42, 45]. The thrombin receptor CD141 was increased in monocytes [41]. CD141 impairs blood coagulation, which, among other mechanisms, could be an additional explanation for thromboembolic complications, especially in CVD patients and COVID-19 [26, 40, 41]. However, this is rather observational, and one can only speculate that different CD141 expressions in both patient groups might be one relevant influencing factor during thromboembolic complications or coagulopathy in SARS-CoV2 infection. The differences in CD141 expression were detected in the early stages of the infection, which might also help identify patients at risk for coagulopathy during the course of viral disease. In addition, the reduced CD19 expression of plasmablasts and B-cell subsets could indicate a lower B-cell receptor signalling [30, 35]. pDCs and cDC subsets showed a more migratory phenotype, as evidenced by their increased expression of CCR7. In contrast, CXCR3 was lowly expressed on neutrophils, mature NK cells, $CD161^+$ T cells, and several $CD4^+$ T-cell subsets, suggesting an impaired migratory capacity. Ligands for CXCR3, CXCL10, and CXCL11 increased and correlated with disease severity [46]. One possible explanation for the reduced CXCR3 expression on many immune cells is downregulation upon ligand binding [47].

Interestingly, naïve $CD4^+$ and $CD8^+$ T cells from severely infected CVD patients expressed more CD95 than those from mildly infected patients, indicating impaired activation due to CD95-mediated inhibition of the T-cell receptor signalling [48]. As with the NK cells [4], predominantly innate immune cells from severely infected CVD patients expressed less CD16 than patients with mild infection. This indicates reduced antibody-dependent cellular cytotoxicity, which impairs the killing of virus-infected cells [31]. In contrast to Georg et al. [49], we could not detect $CD16^+$ activated T cells in severely infected SARS-CoV-2 CVD patients. This discrepancy could be due to differences in the cohorts (all-comers versus CVD patients) and medication before blood sampling (partial medication such as antibiotics or steroids compared with no medication in our study).

CVD patients with pre-existing cardiac and vascular dysfunction may benefit from intensified heart failure and anti-thrombotic therapy before progression to respiratory failure [4]. Since there is currently limited causal therapy for SARS-CoV-2 infection, early identification and treatment of prognostically relevant comorbidities are critical to prevent a fatal course triggered by the disease. Our study has shown that a combination of the abundance of only three immune cells detected in the blood at hospital admission (NKT cells, $CD161^+$ T cells, and intermediate $CD8^+$ effector T cells) is sufficient to distinguish CVD patients with mild from those with severe course of infection. This specific immune signature was independently associated with the assigned severity of COVID-19.

A study from Messing et al. [50] showed that serum IL-10 levels and specific monocyte subsets could serve as effective prognostic biomarkers to predict the clinical outcomes of ICU COVID-19 patients at the time of admission. This study also demonstrated the need for two biomarkers, measured by CYTOF and bead-based immunoassay, to predict disease progression in COVID-19. In contrast to our approach, the sensitivity and specificity of these two biomarkers were lower than those of our three biomarkers, and two methods were required for prediction.

High-risk CVD patients could benefit from intensified monitoring and early anti-inflammatory treatment strategies, thereby

preventing long-term ICU treatment or fatal outcomes. In addition, there were no confounding factors in the OPLS-DA analysis, such as comorbidities, suggesting that the immune signature may serve as an additional and objective tool for more intensive risk assessment of CVD patients with COVID-19 and increased risk of severe disease progression or infection-related disadvantages or complications, respectively.

Data limitations and perspectives

Although we have studied a relatively large cohort of CVD patients with and without SARS-CoV-2 infection and HD, the number of patients with severe courses is limited. Moreover, we are unable to provide data on healthy people without comorbidities, such as diabetes, obesity, etc., who were infected with SARS-CoV-2 as they were not treated in our hospital. Nevertheless, we have emphasised the similarities and differences between our cohort to several studies focusing on SARS-CoV-2 infection in all individuals (regardless of comorbidities) treated at the hospital in the discussion.

We analysed PBMCs after density gradient centrifugation. Therefore, a large part of the neutrophils is lost, which were shown to be crucial for distinguishing between the fatal and non-fatal outcomes of COVID-19 [39]. Moreover, our analyses did not cover the immune response at the infection site.

Our study found that a specific immune signature is related to the severity of COVID-19 in patients with CVD and can predict disease progression on first admission to the hospital. The early determination of the immune signature could enable treating physicians to provide the best possible pharmacological and device-based treatment at an early stage and thus improve clinical outcomes.

In addition, the study demonstrates the relevance of high-dimensional flow cytometry and bioinformatics analysis as a proof-of-principle for detecting an immune signature at the protein level to predict disease progression. Further analyses of a large cohort of nowadays vaccinated patients would be needed for confirmation.

Materials and methods

Study design, participants, and assessment of clinical parameters

From February to April 2020, we prospectively studied a consecutive cohort of 94 non-vaccinated participants at the Department of Cardiology and Angiology of the University Hospital Tübingen, Germany. Of these, 37 consecutive patients with pre-existing CVD and symptomatic, acute SARS-CoV-2 infection (CVD^{+}SARS-CoV-2) were admitted to our emergency department. Twenty patients with pre-existing stable CVD without infections were matched (Tables S1–S3). Thirty-seven healthy donors (HD) served as controls (Table S1). All patients underwent clinical and cardiac assessment, including echocardiography, electrocardiography, concomitant medication, comorbidities, and blood sampling for routine laboratory parameters within 12 h of admission. SARS-CoV-2 infection was diagnosed by RNA detection from nasopharyngeal secretions with real-time reverse transcriptase polymerase chain reaction. Pre-existing CVD was defined as stable coronary artery disease, which had been determined by coronary angiography and diagnosed when there was luminal stenosis of one or more coronary vessels >25–50% diameter before hospital admission. Respiratory failure was defined by a Horovitz index $\leq$ 200mmHg [51]. The inclusion criteria were confirmed CVD with or without SARS-CoV-2 infection and an age $\geq$18. Exclusion criteria were other viral or bacterial infections and malignancies.

Isolation of peripheral blood mononuclear cells

Blood samples of patients with CVD (including SARS-CoV-2 infection) and HD were collected in CPDA monovettes and were processed within 4 h after blood collection. Peripheral blood mononuclear cells (PBMCs) were isolated using SepMate tubes (Stem Cell Technologies) according to the manufacturer's instructions. The blood was diluted 1:1 with PBS, stacked on 15 mL Biocoll separation solution ((1077 g/mL), Biochrom) in a 50 ml tube, and centrifuged at 1200 $\times$ *g* for 10 min without brake at RT. The clear supernatant containing the PBMCs was decanted and washed three times with PBS+2% FCS. PBMCs were frozen as aliquots of 1–2 $\times$ 10^7 cells/mL in RPMI1640 containing 20% FBS and 10% DMSO at −150°C until further use. Using this purification method, the PBMC fraction still contains 0.5–1% low-density granulocyte contamination [19, 52].

Flow cytometry staining

PBMCs were thawed in a water bath at 37°C, and 10 mL RPMI (Sigma) containing 50 KU DNaseI (Merck) were added. Cells were centrifuged at 400 $\times$ *g* for 5 min at RT. The supernatant was discarded, and the cells were resuspended in 5 mL RPMI containing 200 KU DNaseI and incubated for 20 min at 37°C. The cell numbers were determined by trypan blue exclusion using a Neubauer counting chamber. Cells were washed once with PBS, and 3 $\times$ 10^6 cells were stained with LIVE/DEAD fixable blue dead cell stain kit (Thermo Fisher Scientific) according to the manufacturer's instructions (final dilution 1:1000). All following washing and incubation steps were performed with Cell Staining Buffer (BioLegend). Cells were incubated with Human True StainFcX (BioLegend) at RT for 10 min, followed by extracellular staining for 1 h at 4°C using the antibodies listed in Table S4, in a final volume of 100 µL containing 5 µL True-Stain Monocyte Blocker (BioLegend). Cells were washed twice with staining buffer, and at least 1.5 $\times$ 10^6 cells were acquired using an Aurora (Cytek Bioscience) with the SpectroFlow software.

Unmixing was performed in SpectroFlow using cell- or bead-based single-stain controls and unstained cells for autofluorescence subtraction.

We performed a classical gating strategy (Fig. 1) for quality control of the 36-colour panel and unsupervised data analysis described in supplementary material using OMIQ software (Dotmatics). The supporting information provides a detailed description of the data analysis.

Determination of plasma levels of cytokines/chemokines

Two LEGENDPlex (Inflammation Panel 1 and Pro-inflammatory Chemokine Panel; BioLegend) were performed to quantify the chemokine and cytokine concentrations in human plasma. Sixty-nine frozen plasma samples were analysed, consisting of 27 HD, 15 CVD, and 27 SARS-CoV-2-infected CVD patients. The assays were performed according to the manufacturer's manual. A FACS Lyric (BD Biosciences) was used for the measurement. Data analysis was performed with the LEGENDPlex Data Analysis Software (BioLegend).

Statistical analysis

Statistical analyses were performed with GraphPad Prism version 8.0.2 and R software version 4.0. We determined clinical and laboratory baseline characteristics concerning measured immune cell phenotypes, marker expression, and clinical outcome. Continuous variables are expressed as median ± interquartile range (clinical data) or median ± standard deviation (flow cytometry and cytokine data). All datasets were tested for normal distribution using the Shapiro–Wilk normality test. Since all normality tests returned negative, data sets were compared using multiple unpaired two-tailed Mann–Whitney *U* tests for two-group comparisons corrected for multiple comparisons using a false discovery rate. Three-group comparisons were analysed using the Kruskal Wallis non-parametric test with Dunn's (Figures) or Bonferroni (Tables) post-tests. Categorical data are presented as total numbers and proportions and were analysed using a chi-squared test. Correlation calculations between two parameters were performed by Spearman rank correlation coefficient *r*.

To summarise, correlations of essential parameters in CVD patients with and without SARS-CoV-2 infection matrices were generated using Rstudio "Corrplot" displaying correlations of cytokines. Spearman's ρ is coloured, and colour intensity and size are plotted proportionally to correlation coefficients. The "CombiROC" package [32] (http://combiroc.eu/) was used in Rstudio to determine the optimal combination of cell populations to differentiate mild from severe or moderately SARS-CoV-2-infected CVD patients. OPLS-DA [33] was performed using the "MetaboAnalyst" package in RStudio. Comparisons were considered statistically significant if the two-sided *p*-value was <0.05 (* <0.05; ** <0.01; *** <0.001; **** <0.0001).

Acknowledgements: This research was funded by the German Research Foundation (DFG) (grant number: 374031971–TRR 240) and by the Ministry of Science, Research and the Arts of the State of Baden-Württemberg (Long-COVID Funding). The authors thank Felix Herth (Department of Pneumology and Critical Care Medicine, University of Heidelberg) for the critical discussion and the Core Facility Flow Cytometry of the Medical Faculty Tübingen for technical help.
Open access funding enabled and organized by Projekt DEAL.

Conflict of interest statement: The authors declare no commercial or financial conflict of interest.

Author contributions: Conceptualization: Karin Anne Lydia Mueller, Meinrad Paul Gawaz, and Stella E. Autenrieth; methodology: Manina Günter, Carolin Prang, Karin Anne Lydia Mueller, and Sarah Gekeler; formal analysis: Manina Günter, Karin Anne Lydia Mueller, Mathew J. Salazar, Tobias Harm, Stella E. Autenrieth; investigation: Karin Anne Lydia Mueller; resources: Meinrad Paul Gawaz and Stella E. Autenrieth; writing—original draft preparation: Manina Günter, Karin Anne Lydia Mueller, and Stella E. Autenrieth; writing—review and editing: Manina Günter, Karin Anne Lydia Mueller, Mathew J. Salazar, Meinrad Paul Gawaz, and Stella E. Autenrieth; visualization: Manina Günter, Karin Anne Lydia Mueller, and Stella E. Autenrieth; supervision: Stella E. Autenrieth; funding acquisition: Karin Anne Lydia Mueller, Meinrad Paul Gawaz, and Stella E. Autenrieth. All authors have read and agreed to the published version of the manuscript.

Ethics approval statement for human and/or animal studies: The study was approved by the local ethics committee (approval number 240/2018BO2) and conducted in accordance with the 1964 Helsinki Declaration and its later amendments.

Patient consent statement: Written informed consent was obtained from each patient.

Data availability statement: The data that support the findings of this study are openly available in FlowRepository at http://flowrepository.org/, reference number FR-FCM-Z78W.

Peer review: The peer review history for this article is available at https://publons.com/publon/10.1002/eji.202451145

References

1 **Koutsakos, M. and Kedzierska, K.**, A race to determine what drives COVID-19 severity. *Nature*. 2020. **583**: 366–368.

2 **Zhang, X., Tan, Y., Ling, Y., Lu, G., Liu, F., Yi, Z., Jia, X. et al.**, Viral and host factors related to the clinical outcome of COVID-19. *Nature*. 2020. **583**: 437–440.

3 **Thevarajan, I., Nguyen, T. H. O., Koutsakos, M., Druce, J., Caly, L., van de Sandt, C. E., Jia, X. et al.**, Breadth of concomitant immune responses prior to patient recovery: a case report of non-severe COVID-19. *Nat. Med.* 2020. **26**: 453–455.

4 **Kuri-Cervantes, L., Pampena, M. B., Meng, W., Rosenfeld, A. M., Ittner, C. A. G., Weisman, A. R., Agyekum, R. S. et al.**, Comprehensive mapping of immune perturbations associated with severe COVID-19. *Sci. Immunol.* 2020. **5**: eabd7114.

5 **Mathew, D., Giles, J. R., Baxter, A. E., Oldridge, D. A., Greenplate, A. R., Wu, J. E., Alanio, C. et al.**, Deep immune profiling of COVID-19 patients reveals distinct immunotypes with therapeutic implications. *Science*. 2020. **369**: eabc8511.

6 **Long, Q. X., Tang, X. J., Shi, Q. L., Li, Q., Deng, H. J., Yuan, J., Hu, J.-L. et al.**, Clinical and immunological assessment of asymptomatic SARS-CoV-2 infections. *Nat. Med.* 2020. **26**: 1200–1204.

7 **Zhou, F., Yu, T., Du, R., Fan, G., Liu, Y., Liu, Z., Xiang, J. et al.**, Clinical course and risk factors for mortality of adult inpatients with COVID-19 in Wuhan, China: a retrospective cohort study. *Lancet North Am. Ed.* 2020. **395**: 1054–1062.

8 **Mangalmurti, N. and Hunter, C. A.**, Cytokine Storms: Understanding COVID-19. *Immunity*. 2020. **53**: 19–25.

9 **Wolf, D. and Ley, K.**, Immunity and inflammation in atherosclerosis. *Circ. Res.* 2019. **124**: 315–327.

10 **Bahrar, H., Bekkering, S., Stienstra, R., Netea, M. G. and Riksen, N. P.**, Innate immune memory in cardiometabolic disease. *Cardiovasc. Res.* 2023. **119**: 2774–2786.

11 **Swirski, F. K. and Nahrendorf, M.**, Cardioimmunology: the immune system in cardiac homeostasis and disease. *Nature*. 2018. **18**: 1–12.

12 **Woollard, K. J. and Geissmann, F.**, Monocytes in atherosclerosis: subsets and functions. *Nat. Rev. Cardiol.* 2010. **7**: 77–86.

13 **Roy, P., Orecchioni, M. and Ley, K.**, How the immune system shapes atherosclerosis: roles of innate and adaptive immunity. *Nat. Rev. Immunol.* 2022. **22**: 251–265.

14 Cardiology TTF for the management of C of the ES of, **Baigent, C., Windecker, S., Andreini, D., Arbelo, E., Barbato, E. et al.**, ESC guidance for the diagnosis and management of cardiovascular disease during the COVID-19 pandemic: part 2—care pathways, treatment, and follow-up. *Eur. Heart J.* 2021. **43**: 1059–1103.

15 **Xiong, T. Y., Redwood, S., Prendergast, B. and Chen, M.**, Coronaviruses and the cardiovascular system: acute and long-term implications. *Eur. Heart J.* 2020. **41**: 1798–1800.

16 **Chen, C., Zhou, Y. and Wang, D. W.**, SARS-CoV-2: a potential novel etiology of fulminant myocarditis. *Herz*. 2020. **45**: 230–232.

17 **Tay, J. Y., Lim, P. L., Marimuthu, K., Sadarangani, S. P., Ling, L. M., Ang, B. S. P., Chan, M. et al.**, De-isolating COVID-19 suspect cases: a continuing challenge. *Clin. Infect. Dis.* 2020. **71**: ciaa179.

18 **Tang, N., Bai, H., Chen, X., Gong, J., Li, D. and Sun, Z.**, Anticoagulant treatment is associated with decreased mortality in severe coronavirus disease 2019 patients with coagulopathy. *J. Thromb. Haemost.* 2020. **18**: 1094–1099.

19 **Park, L. M., Lannigan, J. and Jaimes, M. C.**, OMIP-069: forty-color full spectrum flow cytometry panel for deep immunophenotyping of major cell subsets in human peripheral blood. *Cytometry Part A*. 2020. **97**: 1044–1051.

20 **McInnes, L., Healy, J., Saul, N. and Großberger, L.**, UMAP: uniform manifold approximation and projection. *J. Open Source Software*. 2018. **3**: 861.

21 **Gassen, S. V., Callebaut, B., Helden, M. J. V., Lambrecht, B. N., Demeester, P., Dhaene, T., Saeys, Y. et al.**, FlowSOM: Using self-organizing maps for visualization and interpretation of cytometry data. Brinkman RR, Aghaeepour N, Finak G, Gottardo R, Mosmann T, Scheuermann RH, editors. *Cytometry B Clin. Cytom*. 2015. **87**: 636–645.

22 **Li, Y., Jiang, S., Li, J., Yin, M., Yan, F., Chen, Y., He, Y. et al.**, Phenotypic changes of peripheral γδ T cell and its subsets in patients with coronary artery disease. *Front. Immunol.* 2022. **13**: 900334.

23 **Touch, S., Assmann, K. E., Aron-Wisnewsky, J., Marquet, F., Rouault, C., Fradet, M., Mosbah, H. et al.**, Mucosal-associated invariant T (MAIT) cells are depleted and prone to apoptosis in cardiometabolic disorders. *FASEB J.* 2018. **32**: 5078–5089.

24 **Shah, A. D., Denaxas, S., Nicholas, O., Hingorani, A. D. and Hemingway, H.**, Neutrophil counts and initial presentation of 12 cardiovascular diseases A CALIBER cohort study. *J. Am. Coll. Cardiol.* 2017. **69**: 1160–1169.

25 **Reizis, B.**, Plasmacytoid dendritic cells: development, regulation, and function. *Immunity*. 2019. **50**: 37–50.

26 **Ferrari, F., Martins, V. M., Teixeira, M., Santos, R. D. and Stein, R.**, COVID-19 and thromboinflammation: is there a role for statins? *Clinics*. 2021. **76**: e2518.

27 **Imai, T., Baba, M., Nishimura, M., Kakizaki, M., Takagi, S. and Yoshie, O.**, The T cell-directed CC chemokine TARC is a highly specific biological ligand for CC chemokine receptor 4*. *J. Biol. Chem.* 1997. **272**: 15036–15042.

28 **Blankenberg, S., Tiret, L., Bickel, C., Peetz, D., Cambien, F., Meyer, J., Rupprecht, H. J. et al.**, Interleukin-18 is a strong predictor of cardiovascular death in stable and unstable angina. *Circulation*. 2002. **106**: 24–30.

29 **Pearson, T. A., Mensah, G. A., Alexander, R. W., Anderson, J. L., Cannon, R. O., Criqui, M., Fadl, Y. Y. et al.**, Markers of inflammation and cardiovascular disease. *Circulation*. 2003. **107**: 499–511.

30 **Wang, K., Wei, G. and Liu, D.**, CD19: a biomarker for B cell development, lymphoma diagnosis and therapy. *Exp Hematol*. 2012. **1**: 36.

31 **Yeap, W. H., Wong, K. L., Shimasaki, N., Teo, E. C. Y., Quek, J. K. S., Yong, H. X., Diong, C. P. et al.**, CD16 is indispensable for antibody-dependent cellular cytotoxicity by human monocytes. *Sci. Rep.* 2016. **6**: 34310.

32 **Mazzara, S., Rossi, R. L., Grifantini, R., Donizetti, S., Abrignani, S. and Bombaci, M.**, CombiROC: an interactive web tool for selecting accurate marker combinations of omics data. *Sci. Rep.* 2017. **7**: 45477.

33 **Boccard, J. and Rutledge, D. N.**, A consensus orthogonal partial least squares discriminant analysis (OPLS-DA) strategy for multiblock Omics data fusion. *Anal. Chim. Acta*. 2013. **769**: 30–39.

34 **Oren, O., Yang, E. H., Molina, J. R., Bailey, K. R., Blumenthal, R. S. and Kopecky, S. L.**, Cardiovascular health and outcomes in cancer patients receiving immune checkpoint inhibitors. *Am. J. Cardiol.* 2020. **125**: 1920–1926.

35 **Laing, A. G., Lorenc, A., Del Molino Del Barrio, I., Das, A., Fish, M., Monin, L., Muñoz-Ruiz, M. et al.**, A dynamic COVID-19 immune signature includes associations with poor prognosis. *Nat. Med.* 2020. **26**: 1623–1635.

36 **Gatti, A., Radrizzani, D., Viganò, P., Mazzone, A. and Brando, B.**, Decrease of non-classical and intermediate monocyte subsets in severe acute SARS-CoV-2 infection. *Cytometry Part A*. 2020. **97**: 887–890.

37 **Koutsakos, M., Rowntree, L. C., Hensen, L., Chua, B. Y., van de Sandt, C. E., Habel, J. R., Zhang, W. et al.**, Integrated immune dynamics define correlates of COVID-19 severity and antibody responses. *Cell Rep Med*. 2021. **2**: 100208.

38 **Mueller, Y. M., Schrama, T. J., Ruijten, R., Schreurs, M. W. J., Grashof, D. G. B., van de Werken, H. J. G., Lasinio, G. J. et al.**, Stratification of hospitalized COVID-19 patients into clinical severity progression groups by immunophenotyping and machine learning. *Nat. Commun.* 2022. **13**: 915.

39 **Wilk, A. J., Lee, M. J., Wei, B., Parks, B., Pi, R., Martínez-Colón, G. J., Ranganath, T. et al.**, Multi-omic profiling reveals widespread dysregulation of

innate immunity and hematopoiesis in COVID-19. *J. Exp. Med.* 2021. **218**: e20210582.

40 **Breton, G., Mendoza, P., Hägglöf, T., Oliveira, T. Y., Schaefer-Babajew, D., Gaebler, C., Turroja, M. et al.**, Persistent cellular immunity to SARS-CoV-2 infection. *J. Exp. Med.* 2021. **218**.

41 **Kvedaraite, E., Hertwig, L., Sinha, I., Ponzetta, A., Myrberg, I. H., Lourda, M., Dzidic, M. et al.**, Major alterations in the mononuclear phagocyte landscape associated with COVID-19 severity. *Proc. Nat. Acad. Sci. U.S.A.* 2021. **118**: e2018587118.

42 **Mueller, K. A. L., Langnau, C., Günter, M., Pöschel, S., Gekeler, S., Petersen-Uribe, Á., Kreisselmeier, K. P. et al.**, Numbers and phenotype of non-classical CD14dimCD16+ monocytes are predictors of adverse clinical outcome in patients with coronary artery disease and severe SARS-CoV-2 infection. *Cardiovasc. Res.* 2020. **117**: 224–239.

43 **Winheim, E., Rinke, L., Lutz, K., Reischer, A., Leutbecher, A., Wolfram, L., Rausch, L. et al.**, Impaired function and delayed regeneration of dendritic cells in COVID-19. *PLoS Pathog.* 2021. **17**: e1009742.

44 **Uranga-Murillo, I., Morte, E., Hidalgo, S., Pesini, C., García-Mulero, S., Sierra, J. L., Santiago, L. et al.**, Integrated analysis of circulating immune cellular and soluble mediators reveals specific COVID19 signatures at hospital admission with utility for prediction of clinical outcomes. *Theranostics*. 2022. **12**: 290–306.

45 **Zhou, R., To, K. K. W., Wong, Y. C., Liu, L., Zhou, B., Li, X., Huang, H. et al.**, Acute SARS-CoV-2 infection impairs dendritic cell and T cell responses. *Immunity*. 2020. **53**: 864–877.e5.

46 **Khalil, B. A., Elemam, N. M. and Maghazachi, A. A.**, Chemokines and chemokine receptors during COVID-19 infection. *Comput. Struct. Biotechnol. J.* 2021. **19**: 976–988.

47 **Meiser, A., Mueller, A., Wise, E. L., McDonagh, E. M., Petit, S. J., Saran, N., Clark, P. C. et al.**, The chemokine receptor CXCR3 is degraded following internalization and is replenished at the cell surface by de novo synthesis of receptor. *J. Immunol.* 2008. **180**: 6713–6724.

48 **Strauss, G., Lindquist, J. A., Arhel, N., Felder, E., Karl, S., Haas, T. L., Fulda, S. et al.**, CD95 co-stimulation blocks activation of naive T cells by inhibiting T cell receptor signaling. *J. Exp. Med.* 2009. **206**: 1379–1393.

49 **Georg, P., Astaburuaga-García, R., Bonaguro, L., Brumhard, S., Michalick, L., Lippert, L. J., Kostevc, T. et al.**, Complement activation induces excessive T cell cytotoxicity in severe COVID-19. *Cell*. 2022. **185**: 493–512.e25.

50 **Messing, M., Sekhon, M. S., Hughes, M. R., Stukas, S., Hoiland, R. L., Cooper, J., Ahmed, N. et al.**, Prognostic peripheral blood biomarkers at ICU admission predict COVID-19 clinical outcomes. *Front. Immunol.* 2022. **13**: 1010216.

51 **DesPrez, K., McNeil, J. B., Wang, C., Bastarache, J. A., Shaver, C. M. and Ware, L. B.**, Oxygenation saturation index predicts clinical outcomes in ARDS. *Chest*. 2017. **152**: 1151–1158.

52 **Schenz, J., Obermaier, M., Uhle, S., Weigand, M. A. and Uhle, F.**, Low-density granulocyte contamination from peripheral blood mononuclear cells of patients with sepsis and how to remove it – a technical report. *Front. Immunol.* 2021. **12**: 684119.

Abbreviations: **CD4$^+$ early-like T$_{em}$**: early-like effector memory CD4$^+$ T cells · **cDC**: conventional dendritic cell · **COVID-19**: coronavirus disease 2019 · **CRP**: C-reactive protein · **CVD**: cardiovascular disease · **HD**: healthy donor · **ILC**: innate lymphoid cell · **MC**: meta cluster · **NKT**: natural killer T cell · **PBMCs**: peripheral blood mononuclear cells · **SARS-CoV-2**: severe acute respiratory syndrome coronavirus type 2 · **SOM**: self-organised map · **UMAP**: uniform manifold approximation and projection

Full correspondence: Prof. Stella Autenrieth, German Cancer Research Centre, Research Group Dendritic Cells in Infection and Cancer, Im Neuenheimer Feld 280, 69120 Heidelberg, Germany
e-mail: stella.autenrieth@dkfz.de

Received: 15/3/2024
Revised: 16/7/2024
Accepted: 19/7/2024
Accepted article online: 26/7/2024